ECAI 2011 - International Conference – 4th Edition
Electronics, Computers and Artificial Intelligence
30 June -2 July, 2011, Piteşti, ROMÂNIA

Smart Antennas Control Circuits for Automotive Communications

David CORDEAU, Jean-Marie PAILLOT
LAII, EA 1219 – University of Poitiers – ENSIP
IUT, 4 avenue de Varsovie, 16021 Angoulême, France
david.cordeau@univ-poitiers.fr, jean.marie.paillot@univ-poitiers.fr

Keywords: Beam steering, smart antenna systems, coupled oscillators, synchronization, design automation, active phase shifter, vector modulators

Abstract. *This paper presents two architectures allowing to perform beam steering and beam forming by controlling the relative amplitudes and phases of the signals applied on each element of a linear antenna array. The first one is based on the use of an array of coupled oscillators operating at 900 MHz. In this case, a CAD tool, which provides the frequency locking region of the coupled oscillators is presented and the application of the proposed tool to beam steering is illustrated. Experimental results of an array of 4 oscillators are then shown. The second architecture uses vector modulators to achieve the required relative amplitude and phase. In this case, noise sensitivity is first studied and simulated to prove the interest of this architecture and experimental results of a prototype including an array of four "patch" antennas controlled by the vector modulators will be presented.*

INTRODUCTION

Omnidirectional antennas are widely used in transmission systems. However, their uniform radiation allows only a small fraction of the radiated power to reach the intended receiver, thus causing an important Electro-Magnetic pollution. Consequently, in an environmental perspective, the ratio of useful power to lost power is inappropriate for a lot of applications. Furthermore, recent researches on the detection algorithms of Angle of Arrival (AOA), like MUSIC or SAGE [1, 2], have opened new perspectives and service capabilities in the field of intelligent transport, for instance, the control-command of public bus or automotive communications. In this case, the transmitter needs first to detect the mobile receiver and then lock its radiation pattern on it while transmitting data on the desired direction. In this context, electronically-steered phased arrays constitute an alternative technology. In such systems, the directional sensitivity of the phased array can be adjusted by controlling the relative amplitudes and phases of the signals applied on each element of the array.
Several solutions, with phase shifters or phase shifterless, are proposed to achieve this electronic modification of the radiation pattern. Indeed, passive phase shifters can be used to perform the phase control. Unfortunately their losses degrade the overall system performances. Other solutions such as Rotman lenses [3] or Butler matrices [4] can also be used especially for beam-steering and switched beam antenna arrays. Concerning the phase-shifterless solutions, Ali Hajimiri and his work group recently proposed an architecture using a polyphase voltage-controlled oscillator, which is able to generate the local oscillator frequency with N phases. In this architecture, all the N phases are conveyed to each antenna via a distribution network. Phase selectors ensure the required phase to each element [5, 6]. In this case, the phase variations are discrete, which does not constitute a problem as

long as the discrimination steps are adequate to the application. Nevertheless, the distribution network of N phases constitutes a real issue here since each path must be forwarded to the phase selector in a symmetrical way.
In this context, this paper presents two different kinds of architecture allowing to perform electronic beam steering by controlling the relative amplitudes and phases of the signals applied on each element of the array. The first one is based on the use of an array of coupled oscillators operating at 900 MHz and the second one is a 2.4 GHz architecture based on vector modulators.
The paper is organized as follows. After a brief review of beam steering of a one dimensional array presented in section 1, the architecture using an array of coupled oscillators will be presented in section 2. In particular, the developed CAD tool that permits to acquire, in a considerably short simulation time, the frequency locking region of the coupled oscillators, in terms of the amplitudes of their output signals and the phase shift between them will be presented. After that, the application of the proposed tool to beam steering will be illustrated and experimental results of an array of 4 oscillators will be shown. In section 3, the architecture using vector modulators as active phase shifters will be described. After a noise sensitivity study, experimental results of a prototype including an array of four "patch" antennas controlled by the vector modulators will be presented.

1. BRIEF REVIEW OF SMART ANTENNA PRINCIPLE

A smart antenna consists of an array of individual radiation elements (elementary patch antennas), which are placed in a particular configuration (linear, circular or matrix). By associating these elementary antennas and by changing the characteristics of the applied signals, the array can present different gains according to the direction of propagation. In this paper, a uniformly spaced linear array of N elementary patch antennas is considered, as shown in Fig.1, where d is the distance between two antennas, and θ is the radiation angle.
In order to study the behavior of this configuration, let us suppose that each elementary antenna is excited by harmonic signals at the same frequency, and multiplied by different complex coefficients:

$$w_i = a_i . e^{j\varphi_i}, \quad i \in [1...N] \tag{1}$$

Let us consider that the relative phase shift applied between two adjacent elements is the same $\Delta\varphi=\varphi_{i+1}-\varphi_i$. For far-field, the total electrical radiated field is the sum of individual fields radiated by each elementary antenna. Thus, the total field is given by the following expression:

$$\vec{E}=\sum_{i=1}^{N}\vec{E_i}=\frac{A.e^{-jkr}}{r}\left[\sum_{i=1}^{N}a_i . e^{j(n-1)(k.d.\sin\theta-\varphi_i)}\right] \tag{2}$$

where A is the electrical field magnitude radiated on each elementary pattern without ponderation, r is the maximum distance between the source and the observation plan and k is the propagation constant.
According to (2), the radiation angle θ for the maximum field amplitude is given by :

$$\theta=\arcsin\left(\frac{\lambda.\Delta\varphi}{2\pi.d}\right) \tag{3}$$

Hence, this angle depends on the relative phase shift applied between two adjacent elements. Furthermore, it could be shown that the optimal distance d separating two antennas is $\lambda/2$. In these conditions, Fig.2 shows the normalized amplitude of radiated field versus the radiation angle θ for different values of $\Delta\varphi$.

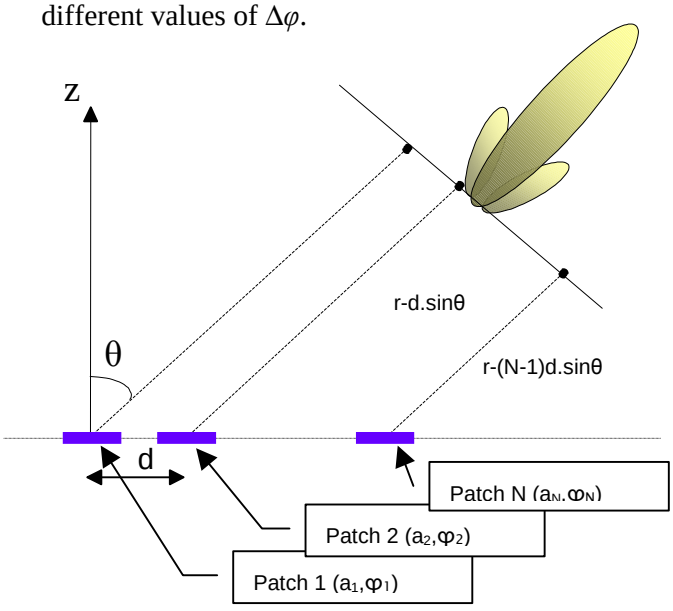

Figure 1. Linear array with N "patch" antennas.

As expected, the relative phase command allows to control the radiation angle and the directivity can be adjusted by varying the number *N* of elements. Indeed, with an eight-elements array, the directivity is equal to 9 dB and the Half Power Beamwidth (HPBW), given by the following expression 2*arccos(1-λ/N.d), is equal to 10°. On the other hand, a control of the amplitude a_i applied on each element can ensure the null formation. For these reasons, to obtain an agile and electronically beam steering, it is essential to master both the amplitudes and the phases applied on each elementary antenna.

2. COUPLED OSCILLATORS ARRAY ARCHITECTURE

In this case, the radiation pattern of the phased antenna array is steered in a particular direction by establishing a constant phase progression throughout the oscillators chain as shown in Figure 3. The required inter-element phase shift can be obtained by detuning the free-running frequencies of the outermost oscillators in the array [7]. The resulting phase shift is then independent of the number of oscillators in the array [8].

CAD Tool

In [9], R. York & J. Lynch derived the equations for the amplitude and phase dynamics of two single-ended Van der Pol oscillators coupled through a RLC circuit. Mathematical manipulations were thus applied to the nonlinear equations describing the locked states of the coupled oscillators proposed in [9].

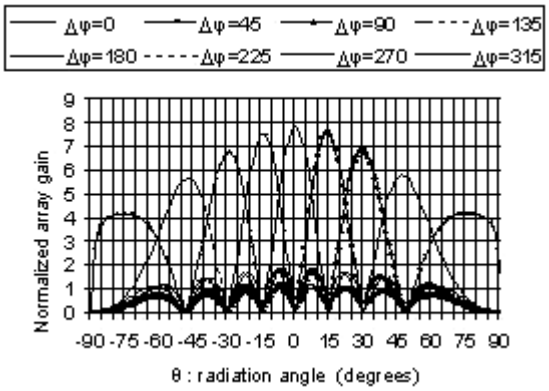

Figure 2. Array gain for eight-elements array, with a measured elementary field of a patch.

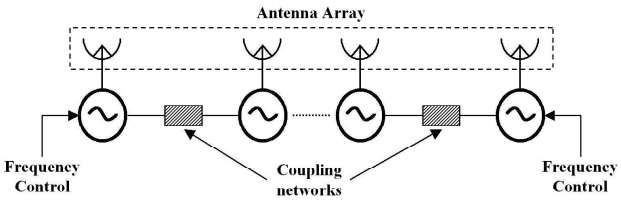

Figure 3. Block diagram of an array of N-coupled oscillators

A reduced system of equations was obtained, thus allowing the elaboration of a CAD tool that permits to acquire, in a considerably short simulation time, the frequency locking region of the coupled oscillators, in terms of the amplitudes of their output signals and the phase shift between them. Indeed, because of the trigonometric and strongly non linear aspect of the equations in [9], thus making their numeric resolution a hard issue, a simpler system of three equations with three unknowns was established in [10]. This system of equations was implemented on Matlab and a CAD tool was developed allowing to obtain the cartography of the locked states of the coupled oscillators.

To do so, the oscillator's architecture used in the array is depicted in Fig. 4. The transistor used is the ATF 35143 PHEMT from Agilent. This transistor is suitable for low noise applications in a frequency range from 450 MHz to 10 GHz. The resonator is made of a parallel RLC circuit with a BBY51 varactor diode allowing to easily control the free-running frequency of the oscillator, according to the required phase shift.

In order to represent the oscillator of Fig. 4 by a negative resistance in parallel with an RLC resonator, Agilent's ADS software was used. From ADS simulation results for one oscillator at the required synchronization frequency, it is then possible to extract the parallel RLC circuit that models the resonator, as well as the parameters a_1 and a_3 of the Van der Pol equation capable of reproducing the behavior of the oscillator's active part. Considering now two oscillators coupled through a series RLC network and using ADS, this system can be reduced into two Van Der Pol oscillators with RLC resonators. Then, the developed CAD tool provides the user with the range of frequencies over which these two oscillators can lock. For instance, for a synchronization frequency of 1.017 GHz, the

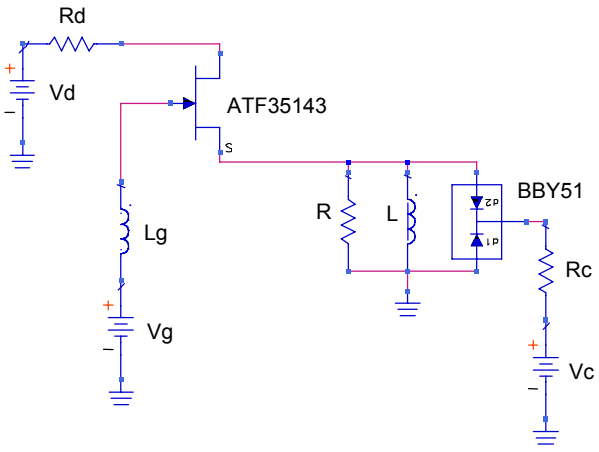

Figure 4. Architecture used for one oscillator of the array

cartography of the oscillators' locked states provided by the CAD tool is presented in Fig. 5. It illustrates the variations of the phase shift $\Delta\phi$ between the two coupled oscillators in function of Δf_{01} and Δf_{02} where $\Delta f_{01} = f_{01}-f_{0c}$ and $\Delta f_{02} = f_{02}-f_{0c}$ with f_{01} and f_{02} the free running frequencies of oscillators 1 and 2 respectively and f_{0c} the resonant frequency of the coupling circuit.

To illustrate the usefulness of this tool for beam steering applications, let us consider that the required main lobe steering angle is $\theta = 15°$ for a distance $d=\lambda/2$. In this case, the relative phase shift which must be applied between two adjacent elements of the antenna array is calculated to be $\Delta\varphi=48°$ using (3). Hence, from the cartography of Fig. 5, one can extract the values of Δf_{01} and Δf_{02} which corresponds to the 48° phase shift required. These were found to be Δf_{01}=19 MHz and Δf_{02}=79 MHz, and consequently, the free-running frequencies to impose are f_{01} = 987.6 MHz for oscillator 1 and f_{02} = 1.048 GHz for oscillator 2, assuming a resonant frequency of f_{0c} = 968.6 MHz for the coupling circuit.

Now, in order to validate our results, Fig . 6 shows a comparison between the phase shift obtained with our CAD tool with the one obtained in simulations using ADS software i.e the circuit simulations of the coupled VCOs and the simulations of their Van der Pol model.

Experimental results

In order to experimentally validate the developed tool, a prototype circuit consisting of 5 coupled oscillators was realized. A photo of the PCB is shown in Fig. 7. In each oscillator circuit, a transistor ATF35143 was used and the varactor diode used in each resonator is the BBY51. Thus, the free running frequency of each oscillator was varied by modifying the command voltage of its varactor diode. The first measurements were performed with two coupled oscillators only. In these conditions, Fig.8 shows a comparison between the measured phase shift and the one given by our CAD tool. The synchronization frequency is 900 MHz in this case and, as shown on Fig. 8, a good agreement is found especially for phase shift values comprised between –10° and +60°.

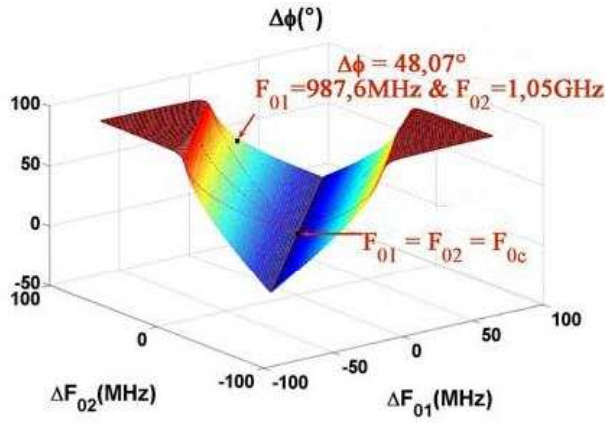

Figure 5. Cartography of the oscillators' locked state provided by the CAD tool

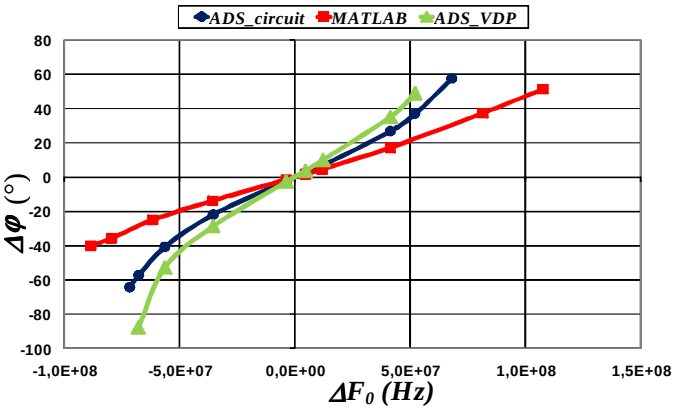

Figure 6. Phase shift versus $\Delta f_0 = f_{01}- f_{02}$

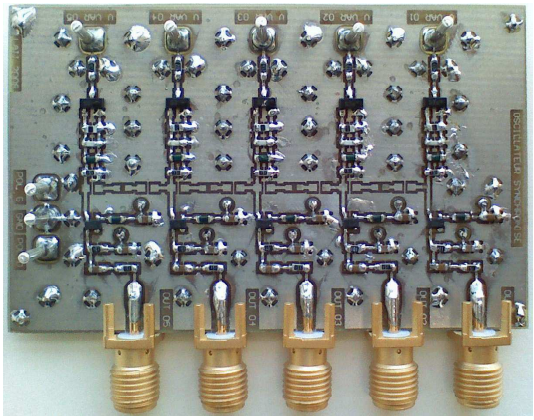

Figure 7. Prototype circuit with 5 coupled oscillators

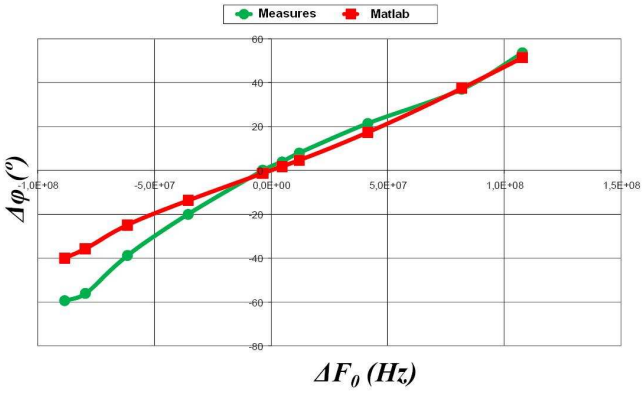

Figure 8. Comparison between measured and calculated phase shift versus Δf_0

3. VECTOR MODULATOR-BASED ACTIVE PHASE SHIFTER ARCHITECTURE

The architecture presented in this section uses vector modulators to achieve the required relative amplitude and phase applied on each antenna.
Two configurations are possible. In the first one, the vector modulator can be placed on the LO path. In this case, the nonlinear and noisy behavior of this active phase-shifter does not affect directly the system performances. On the other hand, this configuration implies an up-conversion before the antenna to transmit or receive the RF signal. Another solution consist in placing the vector modulator directly in the RF path. In these conditions, no up-conversion is required but the IQ modulators noise factors and the non linear behavior can affect the entire system performances. Furthermore, it seems to be interesting to study the degradation of the transmission quality according to the noise that affects the command signals. Therefore, the impact of noisy DC command voltages on the communication system performances will be first presented followed by the experimental results of the 2.4 GHz prototype.

System analysis of the active phase shifter architecture

In order to study the impact of the noise disturbing the command voltages on the communication system performances, simulations using Advanced Design System software of the Agilent Society were done using the architecture shown in Fig.9.
For these simulations, the case of a four “patch” antenna array is considered. The relative phase shift $\Delta\varphi$ applied between two elementary antennas is chosen equal to 100° and a QPSK modulation is chosen for its high sensitivity to phase noise. Symbol rate is set to 11 Mbit/s with a carrier frequency of 2.4 GHz. In this case, Fig. 10.a shows the constellation generated by each vector modulator driven by noisy DC commands when the root mean square (RMS) noise voltage is set to 150 $\mu V/\sqrt{Hz}$. At the receiver, a dual architecture allows one to recover the original constellation. The results are presented in Fig. 10.b. As shown on this figure, the transmission quality is degraded. In order to quantify this degradation, the variation of the error vector magnitude (EVM) against the RMS noise voltages is simulated. Therefore, Fig. 11.a shows the impact of the RMS noise voltage on each antenna for a main lobe steering angles $\theta_{M.L.}$ = 30° (corresponding to $\Delta\varphi$=100° according to (3)). As can be seen from this figure, the EVM is independent of the DC command voltages V_{Im} and $V_{Q\,m}$.
Fig. 11.b shows the EVM evolution always against noise voltages but for different main lobe steering angles $\theta_{M.L.}$. It can be concluded that the EVM hardly changes with the required transmission direction because of the low signal bandwidth to carrier frequency ratio even if, for a noise voltage higher than 2 mV/√Hz, we can observe a slight difference between each curve.

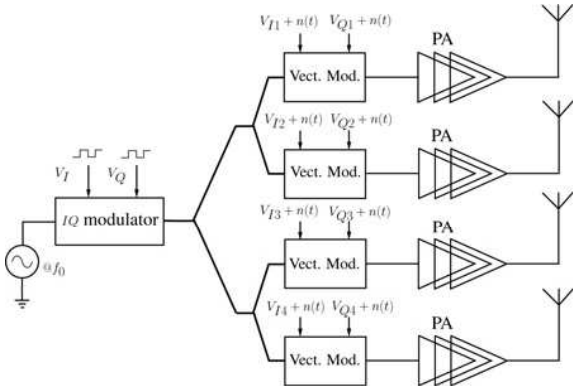

Figure 9. Simplified phased array architecture used in emission

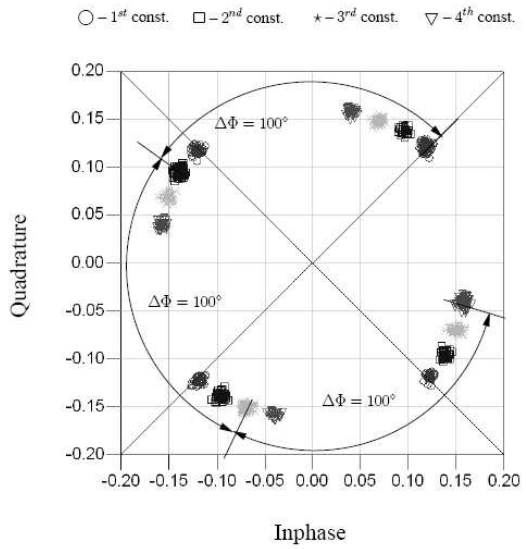

(a)

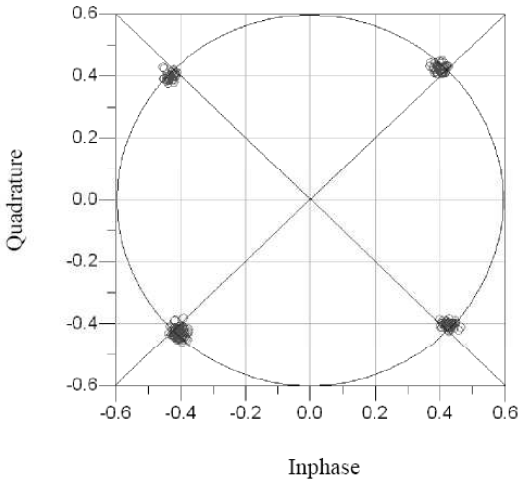

(b)

Figure 10. Emitted (a) and received (b) signal constellation

However, in normal condition of use, the noise voltage level is close to the quantisation noise and thus less than 2 mV/√Hz. Nevertheless, these system simulations prove the necessity to take into account the noise which can be added on the command of the quadrature modulators used as active phase-shifter [11]. Indeed, this noise directly implies transmission perturbations. From this conclusion, the design of a prototype including the antenna array becomes possible. The measurement results are presented in the following sub-section.

Measurement results

A prototype with four "patch" antennas, using discrete components was implemented on a G-10/FR-4 printed circuit board with $\varepsilon_r = 4.6$, tan $\delta = 10^{-2}$ and a conductive layer height $h = 0.35$ µm.

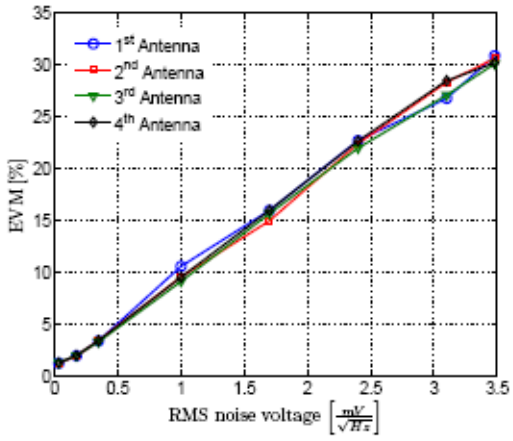

(a)

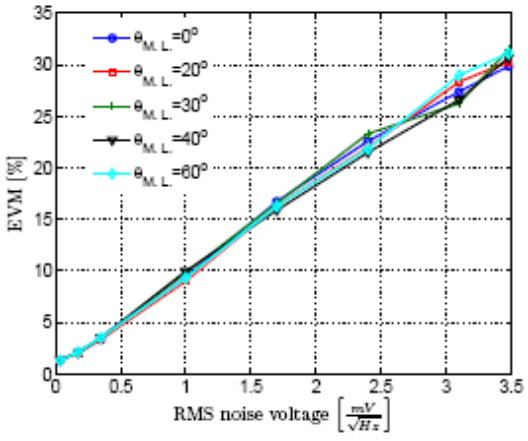

(b)

Figure 11. The EVM against RMS noise voltage: (a) on each antenna, (b) for various depointing angles

The elementary command circuit uses an AD 8394 vector modulator and is followed by an ADL 5330 Voltage Gain Amplifier. Input and output 1:1 transmission line transformers allow the single to differential mode transitions. Four such circuits are driven by an RF signal equally split by a distribution tree. The command circuit output are connected to ”patch” antennas.

Now, in order to verify the ability of the system to perform beamforming, let us consider an array of N=4 identical equidistant antennas ($d = \lambda_0/2$, f_0 = 2.4 GHz) and let us suppose that the direction of the desired signal is θ_u = 30° and the direction of an interference signal is θ_i = -15°. Thus, by using the least mean squares based beamforming algorithm given in [12], the obtained amplitudes A_m and phases ϕ_m which must be applied on each “patch” are given in Table 1. In these conditions, measurements in an anechoic chamber were performed (Fig. 12). V_I an V_Q DC voltages corresponding to the amplitudes and phases given in Table 1 were first applied. An RF signal @ 2.4 GHz and -10 dBm power provided by a ‘Wiltron 360’ 40 GHz network analyser was also applied to the prototype. Fig. 13 shows the theoretical and measured radiation patterns. Theoretical radiation patterns were calculated using Matlab software by multiplying the radiation pattern of one patch antenna with the theoretical array factor. As expected, the measured radiation pattern presents a maximum gain in the 31° direction and a null in the –15° direction. Other radiation pattern measurements at five different main lobe directions are presented in Fig. 14. As shown on these figures, the measured radiation pattern are consistent with the theoretical results.

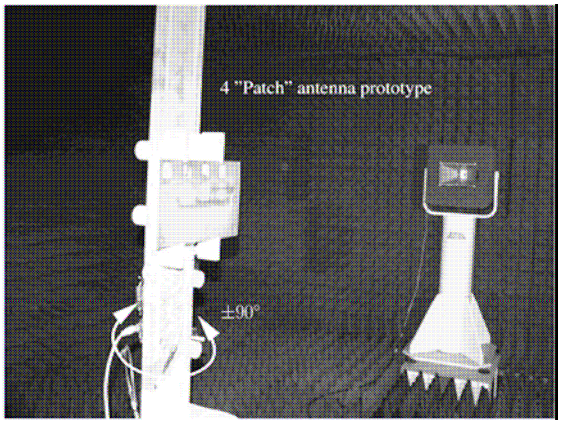

Figure 12. Setup for the radiation pattern measurements in anechoic chamber

TABLE 1. Amplitudes and phases necessary for 4 antennas in the θ_u = 30° and θ_i = -15° scenario

A_m	0.21	0.29	0.29	0.21
ϕ_m	10.51°	-110.4°	176.3°	55.3°

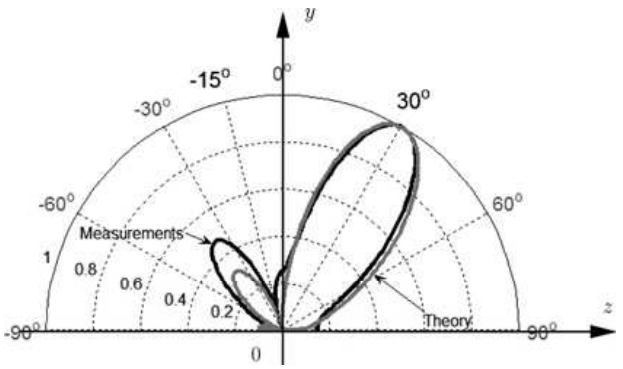

Figure 13. Measured and theoretical normalized radiation pattern in the θ_u = 30° and θ_i = -15° scenario

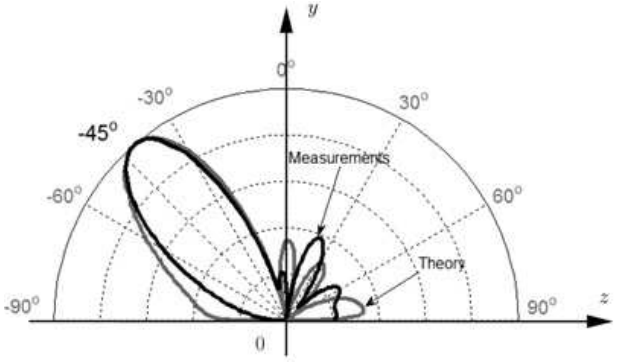

(a)

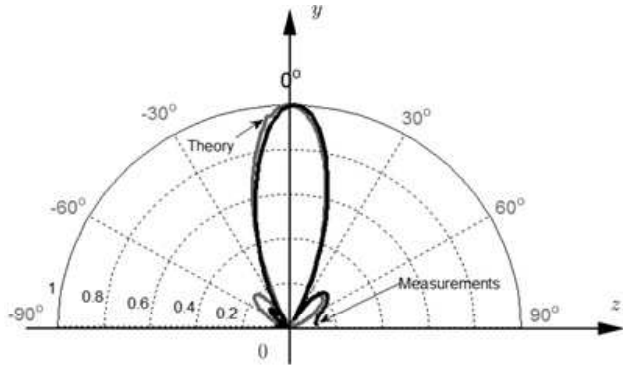

(b)

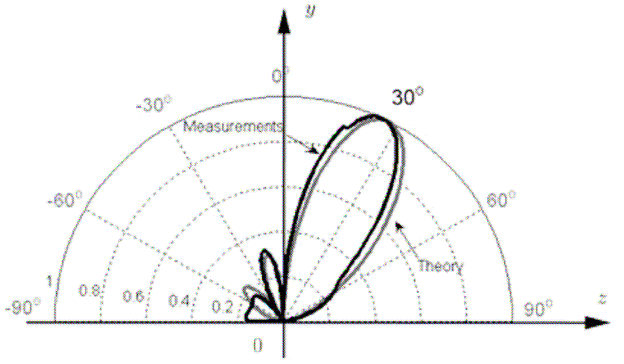

(c)

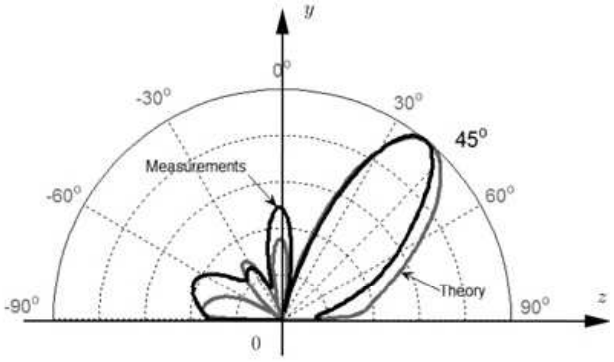

(d)

Figure 14. Measured and theoretical normalized radiation patterns for (a) $\theta_{M.L}$= -45°, (b) $\theta_{M.L}$= 0°, (c) $\theta_{M.L}$= 30°, (d) $\theta_{M.L}$= +45°

CONCLUSION

Two different architectures allowing to perform electronic beam steering and beamforming by controlling the relative amplitudes and phases of the signals applied on each element of a linear antenna array are presented in this paper. For the first one, based on the use of an array of coupled oscillators operating at 900 MHz, a CAD tool was presented and the application of the proposed tool to beam steering was illustrated. Experimental results of a prototype circuit consisting of 5 coupled oscillators were also shown. For a synchronization frequency of 900 MHz, a good agreement was found between the measured and calculated phase shifts especially for values comprised between –10° and +60°. For the second architecture, using vector modulator-based active phase shifters, a system analysis was first performed in order to study the impact of noisy DC command voltages on the system performances. By taking into account these non-ideal behaviors, a 2.4 GHz prototype with four "patch" antennas was implemented and characterized in anechoic chamber. The measured radiation patterns are consistent with the theoretical results.

ACKNOWLEDGEMENTS

The authors thanks the "Poitou-Charentes" region council for the financial support of part of this work.

REFERENCES

[1]. M. Rubsamen and A.B. Gershman "Direction of-arrival estimation for nonuniform sensor arrays: From manifold separation to Fourier domain MUSIC methods", in IEEE Transactions on Signal Processing, Volume 57, Issue 2, 2009, pp. 588. 599.

[2]. B. H. Fleury, P. Jourdan and A. Stucki "High-resolution channel parameter estimation for MIMO application using the SAGE algorithm", in Inernational Zurich Seminar on Broadband Communications, pp. 30–1. 30–9, feb 2002., ETH Zurich.

[3]. Fuchs H.-H., Nussler D.: 'Design of Rotman lens for beamsteering of 94 GHz antenna array', Electron. Lett., 1999, 35, (11), pp. 854–855.

[4]. Tseng C.-H., Chen C.-J., Chu T.-H.: 'A low-cost 60-GHz switched-beam patch antenna array with butler matrix network', IEEE Antennas Wirel. Propag. Lett., 2008, 7, pp. 432–435.

[5]. Guan X., Hashemi H., Hajimiri A.: 'A fully integrated 24-GHz eight-element phase-darray receiver in silicon', IEEE J. Solid-State Circuits, 2004, 39, (12), pp. 2311–2320.

[6]. Natarajan A., Komijani A., Hajimiri A.: 'A fully integrated 24-GHz phased-array transmitter in CMOS', IEEE J. Solid-State Circuits, 2005, 40, (12), pp. 2502–2514.

[7]. P. Liao and R. York, "A new phase-shifterless beam-scanning technique using arrays of coupled oscillators," *IEEE Trans. Microwave Theory Tech.*, vol. 41, pp. 1810–1815, Oct. 1993.

[8]. R. York, "Nonlinear analysis of phase relationships in quasi-optical oscillator arrays," *IEEE Trans. Microwave Theory Tech.*, vol. 41, pp.1799–1809, Oct. 1993.

[9]. J. J. Lynch and R. A. York, "Synchronization of Oscillators Coupled Through Narrow-Band Networks," *IEEE Transactions on Microwave Theory and Techniques*, vol. 49, pp. 237–249, February 2001.

[10]. N. Y. Tohmé, J.M. Paillot, D. Cordeau, P. Coirault, "Analysis of the Frequency Locking Region of Coupled Oscillators Applied to 1-D Antenna Arrays," *European Microwave Conference*, Amsterdam, Holland, pp. 1334-1337, October 2008.

[11]. Tohmé N., Paillot J.-M., Cordeau D., Cauet S., Mahé Y., Ribardière P.: 'A 2.4 GHz 1-dimensional array antenna driven by vector modulators'. IEEE MTT-S Int. Microwave Symp., 2008, pp. 803–806

[12]. FROST III O.L.: 'An algorithm for linearly constrained adaptive array processing', Proc. IEEE, 1972, 60, (8), pp. 926–935